

## LETTERS

# RNA interference screen for human genes associated with West Nile virus infection

Manoj N. Krishnan<sup>1</sup>, Aylwin Ng<sup>4</sup>, Bindu Sukumaran<sup>1</sup>, Felicia D. Gilfoy<sup>5</sup>, Pradeep D. Uchil<sup>3</sup>, Hameeda Sultana<sup>1</sup>, Abraham L. Brass<sup>7</sup>, Rachel Adametz<sup>3</sup>, Melody Tsui<sup>6</sup>, Feng Qian<sup>2</sup>, Ruth R. Montgomery<sup>2</sup>, Sima Lev<sup>8</sup>, Peter W. Mason<sup>5</sup>, Raymond A. Koski<sup>9</sup>, Stephen J. Elledge<sup>7,10</sup>, Ramnik J. Xavier<sup>4\*</sup>, Herve Agaisse<sup>3\*</sup> & Erol Fikrig<sup>1,10\*</sup>

West Nile virus (WNV), and related flaviviruses such as tick-borne encephalitis, Japanese encephalitis, yellow fever and dengue viruses, constitute a significant global human health problem<sup>1</sup>. However, our understanding of the molecular interaction of such flaviviruses with mammalian host cells is limited<sup>1</sup>. WNV encodes only 10 proteins, implying that it may use many cellular proteins for infection<sup>1</sup>. WNV enters the cytoplasm through pH-dependent endocytosis, undergoes cycles of translation and replication, assembles progeny virions in association with endoplasmic reticulum, and exits along the secretory pathway<sup>1–3</sup>. RNA interference (RNAi) presents a powerful forward genetics approach to dissect virus–host cell interactions<sup>4–6</sup>. Here we report the identification of 305 host proteins that affect WNV infection, using a human-genome-wide RNAi screen. Functional clustering of the genes revealed a complex dependence of this virus on host cell physiology, requiring a wide variety of molecules and cellular pathways for successful infection. We further demonstrate a requirement for the ubiquitin ligase CBLL1 in WNV internalization, a post-entry role for the endoplasmic-reticulum-associated degradation pathway in viral infection, and the monocarboxylic acid transporter MCT4 as a viral replication resistance factor. By extending this study to dengue virus, we show that flaviviruses have both overlapping and unique interaction strategies with host cells. This study provides a comprehensive molecular portrait of WNV–human cell interactions that forms a model for understanding single plus-stranded RNA virus infection, and reveals potential antiviral targets.

The host proteins previously reported to facilitate WNV infection (termed host susceptibility factors, HSFs) comprise endosomal transport regulators and vATPase (for entry), eEF1A, TIA-1/TIAR and HMGC1 (for replication), and c-Yes (for secretion)<sup>2,3,7–10</sup>. Other host proteins may reduce WNV infection (termed host resistance factors, HRFs): components of the antiviral IRF3 pathway are known HRFs of WNV infection<sup>11</sup>. In this context, we performed a genome-scale small interfering RNA (siRNA)-based screen silencing 21,121 human genes in HeLa cells to comprehensively identify the cellular proteins associated with the early stages of WNV infection, from viral entry through to the intracellular translation of viral RNA. Defects in the later stages of infection, such as replication, assembly or secretion, were not scored by the assay. The assay involved infection of gene-silenced cells with WNV for 24 h, followed by a microscopy-based quantification of the cells immunostained for viral envelope protein to select the candidate host proteins. The screen was done in two steps: a primary screen using a pool of four siRNAs per gene, followed

by a validation screen, testing each individual siRNA within the pool separately (for the hits selected in the primary screen) to minimize potential off-target hits (Fig. 1a). The details of the assay and screen are described in Methods and Supplementary Fig. 1.

The RNAi screen identified 283 HSFs and 22 HRFs (of which 273 and 21 respectively are novel; Supplementary Tables 1 and 2). The number of HRFs constituted 7% of the total host factors identified. The identification of (1) some of the known HSFs (vATPase, endosomal transport regulators<sup>3</sup>) and HRFs (IRF3; ref. 11) of WNV infection, and (2) multiple components of macromolecular assemblies—for example, vATPase, the endoplasmic-reticulum-associated degradation (ERAD) pathway, focal adhesion complex (FAC)—validated the reliability of our approach and the *in vitro* model. A cellular map summarizing several screen hits classified into cellular compartments and broad functional association categories is provided in Supplementary Fig. 2.

Of the 283 HSFs, 195 (69%) and 193 (68%) could be classified using biological process and molecular function categories, respectively (Fig. 1b, c; Supplementary Tables 3 and 4). There was a significant enrichment of genes regulating intracellular protein trafficking, cell adhesion and processes associated with the transport of ions and biomolecules. The enriched molecular function categories included hydrolases, transporters, ligases, cell adhesion molecules, membrane traffic proteins and synthases. Among the HSFs, 6 RNA-binding proteins (for example, RBPMS), 20 ubiquitination-related proteins (for example, CBLL1), 21 transcription factors (for example, LDB1), 3 C-type lectins (CLEC7A, CLEC4A and CLEC4C) and 5 protocadherins (for example, PCDHB5) were also present. The RNA-binding protein RBPMS was reported as part of a protein network implicated in Purkinje cell degeneration<sup>12</sup>. Strikingly, the current screen also captured seven other members (COIL, PCP4, UBE2I, LDB1, NUMBL, ATXN7L3 and USP6) interacting with RBPMS (Supplementary Figs 3a, b, and 4a, b).

The screen also identified several genes previously implicated in immunity (Supplementary Tables 1 and 2). Immune related HSFs include  $\beta$ -defensins (DEFB118 and DEFB129, Supplementary Fig. 5a), Rnase L inhibitor ABCE1 (refs 13–15; Supplementary Fig. 5b), LY6E, Zap70, TNFSF13B and DUBA (OTUD5). Among the HRFs,  $\alpha$ -defensin DEFA3 and IRF3 are known immune response genes. These findings highlight that defensin family members function as both viral resistance and susceptibility factors<sup>16</sup>. Knockdown of the immunophilin FKBP1B also enhanced WNV infection.

We next determined whether the genes identified from HeLa cells are expressed in tissues targeted by WNV *in vivo* by analysing the

<sup>1</sup>Section of Infectious Diseases, <sup>2</sup>Section of Rheumatology, Department of Internal Medicine, <sup>3</sup>Section for Microbial Pathogenesis, Yale University School of Medicine, New Haven, Connecticut 06520-8031, USA. <sup>4</sup>Center for Computational and Integrative Biology, and Gastrointestinal Unit, Massachusetts General Hospital, Harvard Medical School, Boston, Massachusetts 02114, USA. <sup>5</sup>Department of Pathology, University of Texas Medical Branch, Galveston, Texas 77555, USA. <sup>6</sup>Department of Systems Biology, <sup>7</sup>Department of Genetics, Center for Genetics and Genomics, Brigham and Women's Hospital, Harvard Medical School, Boston, Massachusetts 02115, USA. <sup>8</sup>Department of Neurobiology, Weizmann Institute of Science, Israel. <sup>9</sup>L2 Diagnostics, 300 George Street, New Haven, Connecticut 06511, USA. <sup>10</sup>Howard Hughes Medical Institute, Chevy Chase, Maryland 20815-6789, USA.

\*These authors contributed equally to this work.

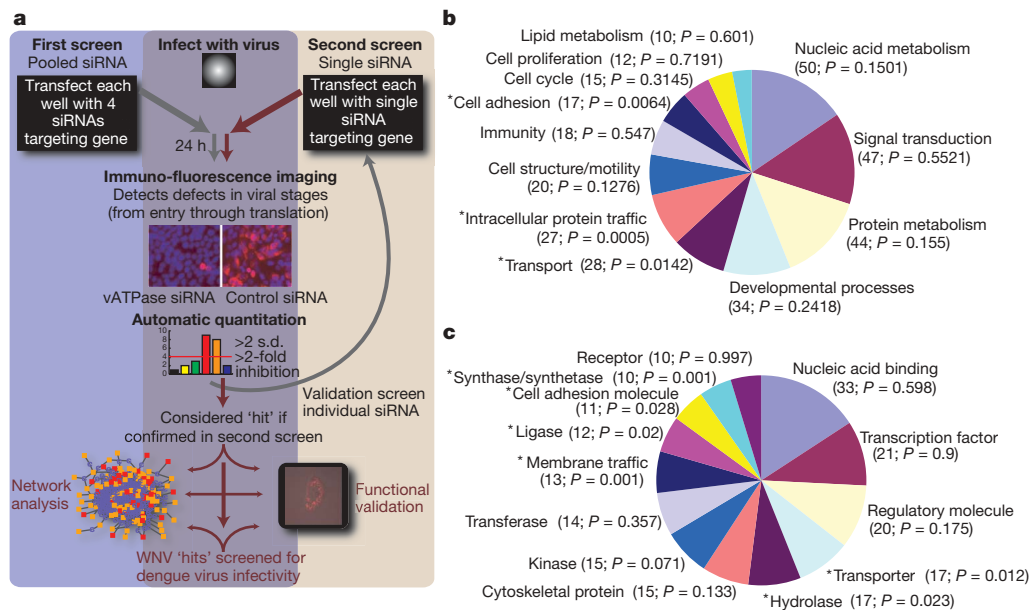


**Figure 1 | RNAi screen and bioinformatics.** **a**, West Nile virus RNAi screen strategy (see text for description). **b**, **c**, Bioinformatics classification of hits into biological process (**b**) and molecular function (**c**) categories. \*Categories found enriched ( $P < 0.05$ ) relative to all the genes examined in the RNAi screen. Only categories with ten or more members are displayed.

expression pattern of the HSFs across 79 tissues (Supplementary Fig. 6). In accordance with the tissue tropism of WNV, 102 (46%) and 64 (29%) HSFs showed enriched expression in immune and central nervous system tissues, respectively (Wilcoxon  $P < 0.05$ ; Supplementary Tables 5 and 6).

Among the 20 ubiquitination-related proteins identified in the screen, the ubiquitin ligase CBLL1 is known to regulate the endocytosis of cell-surface receptors, and therefore we hypothesized that CBLL1 may be involved in the cellular internalization of WNV<sup>17</sup>. CBLL1 silencing resulted in a marked reduction (82%,  $P = 0.05$ ) of WNV-infected cells (Fig. 2a, b; Supplementary Figs 4a, b, and 7a). In order to test whether CBLL1 is involved in WNV entry, we next examined the kinetics of tetramethyl rhodamine iso-thiocyanate (TRITC)-labelled WNV particle internalization into CBLL1 silenced cells. Strikingly, there was a ~20-fold ( $P < 0.05$ ) reduction in the number of virus particles present within CBLL1 silenced cells when analysed from 1 h to 4 h post-incubation (Fig. 2c; Supplementary Fig. 7b). Moreover, virus was seen stuck on the plasma membrane of 17% of CBLL1 silenced cells (Fig. 2d; Supplementary Figs 7b and 8). As expected, CBLL1 silencing did not alter WNV replicon translation (Supplementary Fig. 9a). The virus internalization defect of CBLL1 silenced cells was similar to that observed in cells defective for clathrin dependent endocytosis (CDE), a pathway implicated in WNV entry (Fig. 2d)<sup>2,3</sup>. CDE was ablated by targeting the clathrin adaptor AP3S2, which was also identified in our screen (Supplementary Table 1)<sup>18</sup>. Silencing of the post-entry HSF, vATPase, did not alter the internalization of virus (Fig. 2d). Furthermore, consistent with the involvement of a ubiquitin ligase in WNV entry, depletion of cellular free ubiquitin pool by pretreatment with MG132 (a proteasomal inhibitor) strongly abolished WNV internalization (50-fold,  $P = 0.001$ ) (Fig. 2e; Supplementary Fig. 4b). Notably, proteasome inhibition was also found to interfere with WNV infection at post-internalization steps (Supplementary Fig. 9b). Proteasomal components were also identified in the screen (Supplementary Table 1). Demonstrating WNV specificity, MG132 treatment did not inhibit vesicular stomatitis virus infection (Supplementary Fig. 9c), as reported previously<sup>19</sup>. Collectively, these findings demonstrate that CBLL1 and the proteasome-ubiquitin system are required for the cellular internalization of WNV.

Because the endoplasmic reticulum (ER) is implicated in the intracellular phase of flaviviral life cycle<sup>1</sup>, we examined whether WNV co-opts ER components for infection. Network analysis anchoring on ER proteins revealed the presence of several components of the ERAD pathway among the identified HSFs (Fig. 2f). ERAD comprises

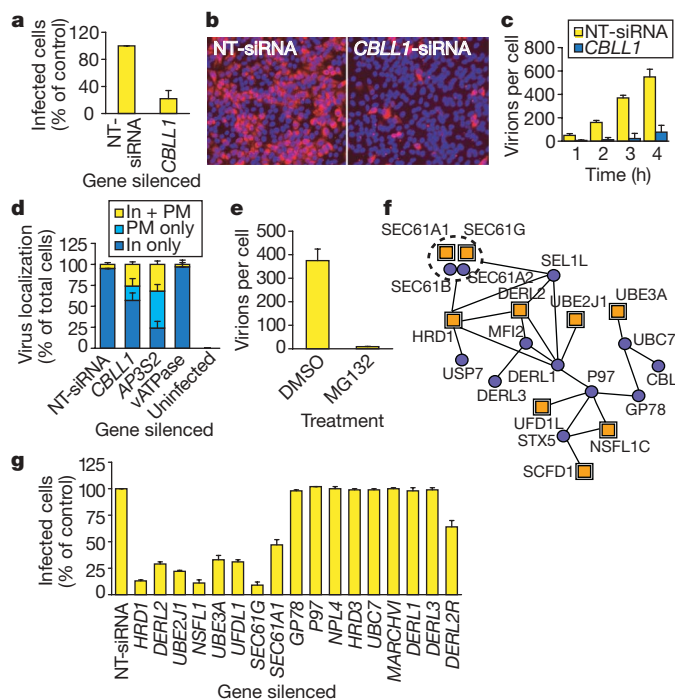


**Figure 2 | CBLL1 and ERAD silencing reduces West Nile virus (WNV) infection.** **a–e**, CBLL1 silenced; **f**, **g**, ERAD silenced. **a**, **b**, CBLL1 silencing reduces WNV immunostained cells (multiplicity of infection, m.o.i.  $\approx 0.3$ , 10 $\times$ , Zeiss). Red, virus; blue, nucleus; NT, non-targeting control siRNA. **c**, Time-course analysis showing reduced internalization of TRITC-WNV (m.o.i.  $\approx 100$ ) into CBLL1 silenced cells. **d**, Localization of TRITC-WNV within CBLL1 silenced cells (percentage of total cells showing the phenotypes, 20 images, ~6 cells each). Plasma membrane alone (PM only), inside the cell (In only), and both PM and inside (In+PM). AP3S2 and vATPase were controls (see text). **e**, MG132 reduces WNV internalization (m.o.i.  $\approx 100$ ). **f**, ERAD network. Yellow squares, hits; blue circles, other host proteins within the network neighbourhood. Dotted line, complexes. **g**, ERAD silencing reduces WNV infection (m.o.i.  $\approx 0.3$ ). DERL2R is an RNAi resistant mutant of DERL2. For **a** and **g**, the percentage of infected control NT-siRNA cells ( $\sim 30\%$ ) was set at 100% and used to normalize the percentage infection of siRNA-treated cells (from six fields of  $\sim 8,000$  cells). Values for **c** and **e** are the number of virus particles per cell (mean of 20 cells). Results are mean  $\pm$  s.d. from a representative experiment performed in triplicate.

more than ten proteins that retro-transport misfolded proteins from ER to the proteasome<sup>20</sup>. Silencing of several key components or interactors of ERAD (*HRD1*, *DERL2*, *UBE2J1/UBC6*, *UBE3A*, *SEC61G*, *SEC61A1*, *UFDIL* and *NSFL1C*), but not other ERAD components (for example, *DERL1*, *DERL3*, *HRD3*, *NPL4* and *p97*), reduced WNV infection up to 89% (Fig. 2g; Supplementary Fig. 4a, b). ERAD was not required for human immunodeficiency virus 2 infection (Supplementary Fig. 10a), highlighting specificity between different viruses. To further validate these results, reduction of viral infection due to silencing of *DERL2* was rescued by transfection with an siRNA-resistant silent mutation-containing variant of *DERL2* (Fig. 2g; Supplementary Fig. 10b). We also identified the recently reported ERAD component *BCAP31* as an HSF<sup>21</sup>. Functional studies revealed that ERAD is not involved in WNV internalization, endosomal transport<sup>2</sup>, or RNA translation; however, there was ~10% reduction in the secretion of progeny virions in ERAD silenced cells (Supplementary Fig. 11a–d, respectively). Interestingly, the simian virus 40 has been shown recently to require the ERAD components *DERL1* and *SEL1L* for uncoating<sup>22</sup>. Together, these results indicate that WNV infection requires a subset of ERAD components at a post-internalization step.

Among the genes whose knockdown enhanced WNV infection, the strongest phenotype was observed when *MCT4* (*SLC16A4*), a plasma membrane transporter of monocarboxylic acids<sup>23</sup>, was silenced. Three of the four tested siRNAs targeting *MCT4* resulted in a 10-fold ( $P = 0.01$ ) increase in WNV infected cells at 24 h (Fig. 3a, b; Supplementary Fig. 4a, b). A quantitative PCR-based time-course analysis of the viral genomic RNA (plus-strand) revealed a similar rate of WNV particle internalization into both *MCT4*-repressed and control cells (Fig. 3c). However, replication started at  $\leq 9$  h post infection in *MCT4*-silenced cells, whereas in control cells it was delayed until after 12 h (Fig. 3c). Consistent with this, *MCT4* silenced cells (1) had 3, 10, 12 and 18 times ( $P < 0.05$ ) more viral plus-strand RNA at 9 h, 12 h, 15 h and 24 h post infection, respectively (Fig. 3c); (2) immuno-stained for WNV antigens at 9 h (not detectable in control cells until after 12 h; Fig. 3d), and (3) secreted progeny virions by 12 h, whereas control cells did not (Fig. 3e). However, importantly, replication of viral genomic RNA introduced directly to the cytoplasm bypassing the entry stages was not affected by *MCT4* silencing (Supplementary Fig. 12). Collectively, these observations show that the functional activity of *MCT4* delays the temporal transition into the replication phase of endocytosed WNV particles.

We next examined whether the host cell interaction strategies are similar between different members of the genus *Flavivirus* by investigating the effect of silencing all the identified WNV HSFs and HRFs in

HeLa cells infected by dengue virus 2 (DENV). We determined that 30 h post-infection of DENV is comparable to the 24 h infection of WNV (Supplementary Fig. 1a, b). Silencing of 36% of the WNV HSFs reduced DENV infection, including previously implicated vATPase and *UBE2I* (Supplementary Table 1)<sup>3,24</sup>. In contrast, all the 22 WNV HRFs increased DENV infection (Supplementary Table 2). Further supporting pathogen specificity, only five of the host factors impacting WNV infection altered HIV-2 infection (not shown).

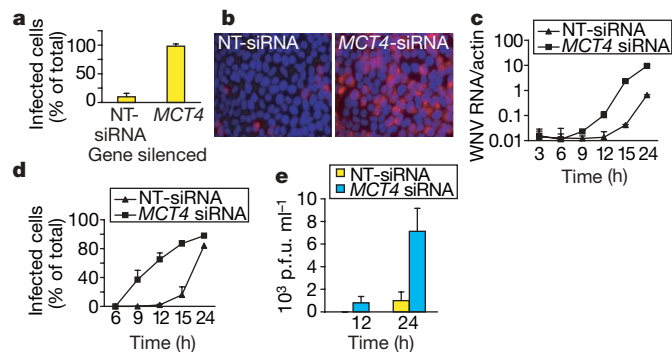


**Figure 3 | *MCT4* silencing enhances WNV replication.** **a, b**, *MCT4* silencing increases the number of WNV immunostained cells (m.o.i.  $\approx 0.3$ ,  $10 \times$ , Zeiss). Red, virus; blue, nucleus. **c**, qPCR of WNV RNA levels in control NT-siRNA and *MCT4* silenced cells (ng viral RNA / ng  $\beta$ -actin). **d**, Immunostaining for WNV E-protein in *MCT4* silenced cells. **e**, WNV secretion from *MCT4* silenced cells, expressed as plaque forming units per ml (p.f.u. ml<sup>-1</sup>). Values in **a** and **d** are percentage of total cells immunostained for WNV (six images having  $\sim 1,000$  cells each). Results are mean  $\pm$  s.d. from a representative experiment performed in triplicate.

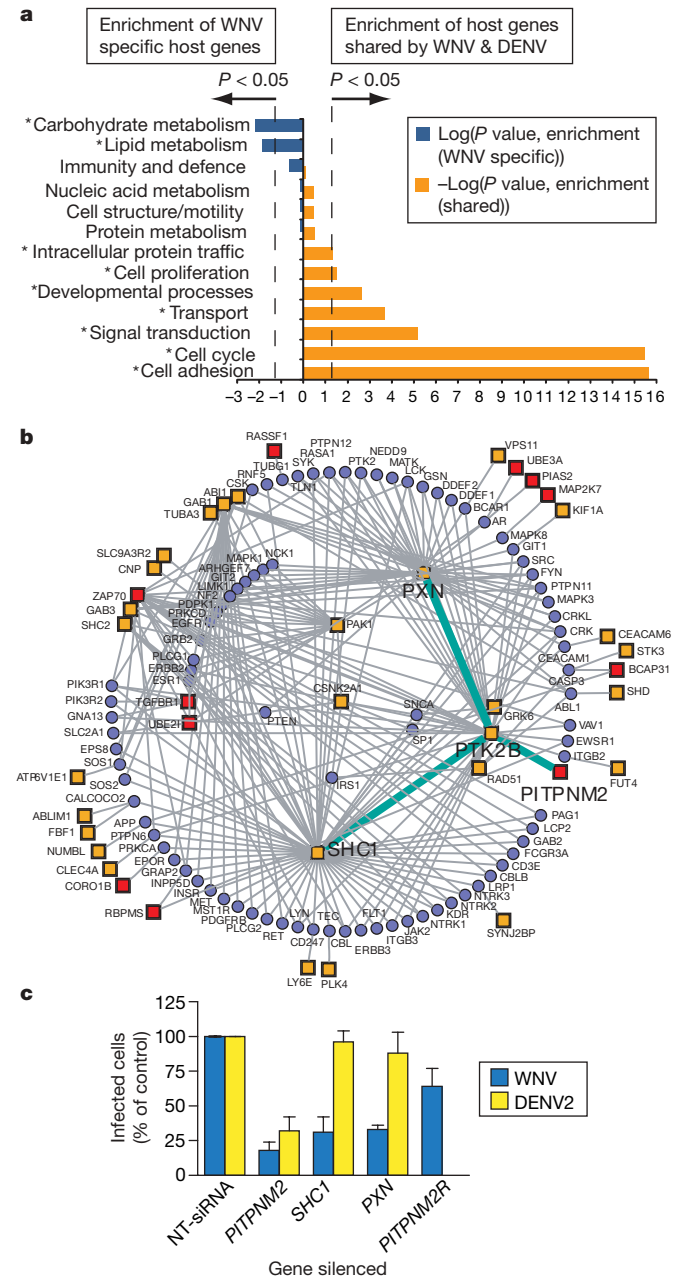


**Figure 4 | Interaction of West Nile virus (WNV) and dengue virus (DENV) with host cells.** **a**, Classification into biological process categories of HSFs common to both WNV and DENV or specific to WNV. \*Categories found enriched ( $P < 0.05$ ) relative to all identified HSFs. **b**, Focal adhesion complex (FAC) network. Cyan line connects the core proteins; yellow squares, WNV specific HSFs; red squares, WNV and DENV shared HSFs; blue circles, other host proteins within the network neighbourhood. **c**, Effect of silencing of *PXN*, *SHC1* and *PITPNM2* on WNV and DENV infection (the percentage of infected control NT-siRNA cells ( $\sim 30\%$ ) was set at 100% and used to normalize the percentage infection of siRNA-treated cells (from six fields of  $\sim 8,000$  cells). *PITPNM2R* indicates an RNAi-resistant mutant of *PITPNM2*. Results are mean  $\pm$  s.d. from a representative experiment performed in triplicate.

An assessment of enrichment for biological process categories revealed significant over-representation ( $P < 0.05$ ) of seven key processes in which HSFs are targeted by both WNV and DENV (Fig. 4a), relative to their representation among all HSFs identified. We selected three pathways—ERAD, FAC and histone deacetylase (HDAC)—to compare the conservation between WNV and DENV. There was a near-complete overlap of ERAD component usage shared by both WNV and DENV, with the single exception of HRD1 (Supplementary Fig. 13a). Silencing of 4 genes constituting the FAC core (for example, *PXN*, *SHC1*, *PITPNM2* and *PTK2B*), and 33 interactors, reduced WNV infection (Fig. 4b, c; Supplementary Fig. 4a, b)<sup>25</sup>. Reduction of WNV infection in *PITPNM2* silenced cells was also rescued with an siRNA resistant *PITPNM2* mutant (Supplementary Fig. 13b). Notably, only one core FAC component (*PITPNM2*) and 11 interactors reduced DENV infection (Fig. 4b, c). Among the nine HDAC components associated with WNV infection, four were required for DENV (Supplementary Fig. 13c). These examples indicate that WNV and DENV may have evolved different sensitivities in their interaction with host proteins, and this may be reflected in the differences in their biology.

In summary, this study portrays a comprehensive genome-scale map of human proteins and cellular pathways affecting the outcome of flavivirus–host cell interactions, and presents a potentially useful resource for further studies. Furthermore, these results may provide insights into the molecular differences in the pathogenesis of related flaviviruses, and reveal potential flaviviral therapeutic targets.

## METHODS SUMMARY

**RNAi screen.** Any gene for which a minimum of two siRNAs reduced (HSF) or increased (HRF) the percentage of infected cells by  $\geq 2$ -fold, and the fold change was  $\geq 2$  times the standard deviation (s.d.) of the percentage of control cells infected, was scored as a hit. Gene silencing that resulted in a cell number decrease  $\geq 2$  times the s.d. (of controls) was considered toxic and excluded.

**Immunofluorescence assay sensitivity determination.** As positive controls to determine whether the immunofluorescence assay (IFA) can detect changes in viral replication, the previously reported WNV replication impacting host gene *HMGCR* was silenced (Supplementary Fig. 1c, d); and to test whether IFA can detect changes in viral translation, host translation machinery was arrested by cycloheximide (Supplementary Fig. 1e). Anti-WNV siRNA was also used as a positive control (Supplementary Table 9). Results showed that the IFA was sensitive enough to detect changes in viral RNA translation, but not later stages such as replication.

**Bioinformatic analysis.** Genes were categorized using the PANTHER classification system<sup>26</sup>. Enrichment was analysed using the hypergeometric probability distribution. For tissue expression analysis, microarray data files were obtained from the Novartis GNF human expression atlas version 2 resource<sup>27</sup>. The protein network constructions used interaction data from the Human Protein Reference Database (HPRD)<sup>28</sup>, the Biomolecular Interaction Network Database (BIND)<sup>29</sup> and the Ingenuity pathways database (Mountainview, CA), supplemented with functional information from the literature.

**Full Methods** and any associated references are available in the online version of the paper at [www.nature.com/nature](http://www.nature.com/nature).

Received 23 March; accepted 26 June 2008.

Published online 6 August 2008.

- Brinton, M. A. The molecular biology of West Nile Virus: A new invader of the western hemisphere. *Annu. Rev. Microbiol.* **56**, 371–402 (2002).
- Chu, J. J. & Ng, M. L. Infectious entry of West Nile virus occurs through a clathrin-mediated endocytic pathway. *J. Virol.* **78**, 10543–10555 (2004).
- Krishnan, M. N. *et al.* Rab 5 is required for the cellular entry of dengue and West Nile viruses. *J. Virol.* **81**, 4881–4885 (2007).
- Brass, A. L. *et al.* Identification of host proteins required for HIV infection through a functional genomic screen. *Science* **319**, 921–926 (2008).
- Ng, T. I. *et al.* Identification of host genes involved in hepatitis C virus replication by small interfering RNA technology. *Hepatology* **45**, 1413–1421 (2007).
- Pelkmans, L. *et al.* Genome-wide analysis of human kinases in clathrin- and caveolae/raft-mediated endocytosis. *Nature* **436**, 78–86 (2005).
- Davis, W. G., Blackwell, J. L., Shi, P. Y. & Brinton, M. A. Interaction between the cellular protein eEF1A and the 3'-terminal stem-loop of West Nile virus genomic RNA facilitates viral minus-strand RNA synthesis. *J. Virol.* **81**, 10172–10187 (2007).

- Emara, M. M. & Brinton, M. A. Interaction of TIA-1/TIAR with West Nile and dengue virus products in infected cells interferes with stress granule formation and processing body assembly. *Proc. Natl Acad. Sci. USA* **104**, 9041–9046 (2007).
- Hirsch, A. J. *et al.* The Src family kinase c-Yes is required for maturation of West Nile virus particles. *J. Virol.* **79**, 11943–11951 (2005).
- Mackenzie, J. M., Khromykh, A. A. & Parton, R. G. Cholesterol manipulation by West Nile virus perturbs the cellular immune response. *Cell Host Microbe* **2**, 229–239 (2007).
- Fredericksen, B. L., Smith, M., Katze, M. G., Shi, P. Y. & Gale, M. Jr. The host response to West Nile Virus infection limits viral spread through the activation of the interferon regulatory factor 3 pathway. *J. Virol.* **78**, 7737–7747 (2004).
- Lim, J. *et al.* A protein-protein interaction network for human inherited ataxias and disorders of Purkinje cell degeneration. *Cell* **125**, 801–814 (2006).
- Mashimo, T. *et al.* A nonsense mutation in the gene encoding 2'-5'-oligoadenylate synthetase/L1 isoform is associated with West Nile virus susceptibility in laboratory mice. *Proc. Natl Acad. Sci. USA* **99**, 11311–11316 (2002).
- Samuel, M. A. *et al.* PKR and RNase L contribute to protection against lethal West Nile Virus infection by controlling early viral spread in the periphery and replication in neurons. *J. Virol.* **80**, 7009–7019 (2006).
- Scherbik, S. V., Paranjape, J. M., Stockman, B. M., Silverman, R. H. & Brinton, M. A. RNase L plays a role in the antiviral response to West Nile virus. *J. Virol.* **80**, 2987–2999 (2006).
- Teclé, T., White, M. R., Gantz, D., Crouch, E. C. & Hartshorn, K. L. Human neutrophil defensins increase neutrophil uptake of influenza A virus and bacteria and modify virus-induced respiratory burst responses. *J. Immunol.* **178**, 8046–8052 (2007).
- Fujita, Y. *et al.* Hakai, a c-Cbl-like protein, ubiquitinates and induces endocytosis of the E-cadherin complex. *Nature Cell Biol.* **4**, 222–231 (2002).
- Dell'Angelica, E. C. *et al.* AP-3: An adaptor-like protein complex with ubiquitous expression. *EMBO J.* **16**, 917–928 (1997).
- Khor, R., McElroy, L. J. & Whittaker, G. R. The ubiquitin-vacuolar protein sorting system is selectively required during entry of influenza virus into host cells. *Traffic* **4**, 857–868 (2003).
- Meusser, B., Hirsch, C., Jarosch, E. & Sommer, T. ERAD: The long road to destruction. *Nature Cell Biol.* **7**, 766–772 (2005).
- Wakana, Y. *et al.* Bap31 is an itinerant protein that moves between the peripheral ER and a juxtannuclear compartment related to ER-associated degradation. *Mol. Biol. Cell* **19**, 1825–1836 (2008).
- Schelhaas, M. *et al.* Simian Virus 40 depends on ER protein folding and quality control factors for entry into host cells. *Cell* **131**, 516–529 (2007).
- Halestrap, A. P. & Price, N. T. The proton-linked monocarboxylate transporter (MCT) family: Structure, function and regulation. *Biochem. J.* **343**, 281–299 (1999).
- Chiu, M. W., Shih, H. M., Yang, T. H. & Yang, Y. L. The type 2 dengue virus envelope protein interacts with small ubiquitin-like modifier-1 (SUMO-1) conjugating enzyme 9 (Ubc9). *J. Biomed. Sci.* **14**, 429–444 (2007).
- Hanks, S. K., Ryzhova, L., Shin, N. Y. & Brabek, J. Focal adhesion kinase signaling activities and their implications in the control of cell survival and motility. *Front. Biosci.* **8**, d982–d996 (2003).
- Mi, H. *et al.* The PANTHER database of protein families, subfamilies, functions and pathways. *Nucleic Acids Res.* **33**, D284–D288 (2005).
- Su, A. I. *et al.* A gene atlas of the mouse and human protein-encoding transcriptomes. *Proc. Natl Acad. Sci. USA* **101**, 6062–6067 (2004).
- Mishra, G. R. *et al.* Human protein reference database — 2006 update. *Nucleic Acids Res.* **34**, D411–D414 (2006).
- Bader, G. D., Betel, D. & Hogue, C. W. BIND: The Biomolecular Interaction Network Database. *Nucleic Acids Res.* **31**, 248–250 (2003).

**Supplementary Information** is linked to the online version of the paper at [www.nature.com/nature](http://www.nature.com/nature).

**Acknowledgements** The human genome RNAi library was made available through the support of the New England Regional Center of Excellence in Biodefense and Emerging Infectious Disease (U54AI057159). The screening was performed at the ICCB-Longwood screening facility (Harvard Medical School). We thank B. Lindenbach for suggestions and Y. Benita for illustrations. We thank L2 Diagnostics for providing the anti-WNV antibody. This work was supported by the NIH. A.N. is supported by a fellowship award from the Crohn's and Colitis Foundation of America. R.J.X. is supported by the NIH (AI062773) and by CCIB development funds. F.D.G. was supported by an NIH training grant in Emerging and Tropical Infectious Diseases (AI07526); portions of this work were supported by a grant from NIAID to P.W.M. through the WRCE (NIH U54 AI057156). E.F. and S.J.E. are Investigators of the Howard Hughes Medical Institute.

**Author Contributions** M.N.K., H.A. and E.F. designed the experiments; M.N.K., B.S., E.F. and R.A. performed the screen; M.N.K., B.S., R.A.K., A.L.B., S.J.E. and H.A. analysed the data; M.N.K. and H.S. performed validations; P.D.U. designed microscopy; F.D.G. and P.W.M. designed replicon experiments; S.L. provided *PITPNM2* cDNA; A.N. and R.J.X. performed bioinformatics analyses; and M.N.K., H.A., A.N., R.J.X. and E.F. co-wrote the paper.

**Author Information** Reprints and permissions information is available at [www.nature.com/reprints](http://www.nature.com/reprints). Correspondence and requests for materials should be addressed to E.F. (erol.fikrig@yale.edu).

## METHODS

**WNV RNAi screen and candidate protein selection criteria.** A library of 21,121 siRNA pools targeting human genome (Dharmacon siARRAY siRNA Library, Human Genome, G-005000-05, Thermo Fisher Scientific) was used. For both the primary and validation screens, HeLa cells (384-well format) were transfected (using Dharmafect 1, Dharmacon) in duplicates with siRNA (50 nM) for 72 h, infected for 24 h with West Nile virus (WNV strain 2471) or 30 h with dengue virus 2 (DENV New Guinea C strain), fixed in 4% paraformaldehyde, immunostained with antibodies detecting viral E-proteins (TRITC labelled, anti-WNV-E antibody developed in horse, or monoclonal anti-DENV-E, Chemicon), and imaged by fluorescence microscopy (Molecular Devices, 4× magnification) using a TRITC filter for virus and DAPI filter for nuclei. Infection was done at an m.o.i. of 0.3 for both WNV and DENV. Generally, infection was in the range of 20–30% for both WNV and DENV. As positive control of infection reduction due to gene silencing, endosomal proton pump vATPase was silenced. Cell number per well was in the range 7,000–9,000. The percentage infection was relatively linear in the cell number range in which the screen was performed (Supplementary Fig. 1f). Each 384-well plate had additional control wells with a non-targeting control siRNA (siCONTROL non-targeting siRNA, Dharmacon) (for determining the general effect of siRNA transfection on infection), siRNA targeting *PLK-1* whose silencing kills the cells (for determining general knockdown efficiency), fluorescently labelled non-targeting control siRNA (for determining transfection efficiency), and wells with neither transfection reagent nor siRNA. Quantification of the effect of gene silencing on viral infection was done using the software Metamorph (Molecular Devices), which counted cells that were immuno-stained versus non-stained for virus antigen. Based on the infection kinetics and infection inhibition by the silencing of a host gene known to be required for the infection of both WNV and DENV (vATPase, Supplementary Fig. 1b), we defined an infection reduction of twofold or greater at 24 h for WNV or 30 h for DENV as the threshold for hit selection. Silencing of vATPase resulted in a reduction of infection of  $2.9 \pm 0.3$  fold compared to the controls for WNV or  $2.7 \pm 0.4$  for DENV (Supplementary Fig. 1b).

**Cell lines and virus propagation.** Gene silencing and infection studies were done on low passage HeLa (ATCC no. CCL-2.1) cells maintained in DMEM supplemented with 10% fetal bovine serum. West Nile virus (strain 2471, gift of J. Anderson), and dengue 2 virus (New Guinea C strain, gift of A. de Silva) viruses were grown on vero (ATCC no. CRL-1586) or C6/36 (ATCC no. CRL-1660) cells, respectively.

**Gene knockdown verification, RNAi resistant mutant generation and phenotype rescue.** For the quantitation of the target transcript reduction, pooled siRNAs corresponding to the tested genes were transfected (50 nM) to cells (or cells pre-transfected with cDNAs of genes) in 48-well plates for 3 days, total RNA was isolated using the RNeasy kit (Qiagen), and cDNA was prepared using the iScript kit (Biorad). Quantitative PCR (qPCR) was performed by using Sybergreen reagent (Biorad). The primers used were given in the Supplementary Table 7. To generate RNAi resistant variants of genes, four silent mutations each were introduced into those sequences of *DERL2* and *PITPNM2* where siRNA binds (in the expression vector pCDNA6.2 with V5 tag), using QuickChange Mutagenesis kit (Stratagene) (Supplementary Table 7 shows the mutagenesis primer sequences). HeLa cells transfected separately with wild type or mutant copies of the genes were selected for 8 days using blasticidin, treated with siRNA for 72 h, and either WNV infection assay or western blot (for knock down and rescue verification) was performed. Six random fields of fluorescent images (10× objective, Zeiss Axiovert 200M) of WNV infected mutant versus wild type gene expressing cells were counted to quantify and assess the rescue of viral infection by mutant genes. For western blot, cells were lysed in 1% 50 mM Tris-HCl, 150 mM NaCl and Triton X-100. Western blot was performed to verify the extent of knockdown and rescue of *DERL2* and *PITPNM2* using anti-V5 antibodies (Invitrogen). Anti-CBL1 antibody was obtained from Abcam.

**Cytotoxicity.** Cytotoxic effects of gene silencing and MG132 treatments were determined using LDH release assay kit (Roche). Supernatants of gene silenced cells were harvested at 3 days post-transfection or 1–24 h post treatment for compounds, and assayed for LDH release according to manufacturer's protocol.

**Viral RNA transfection and secretion studies.** Two kinds of studies were done using viral genomic RNA transfection: (1) determination of the effect of gene silencing on viral RNA translation, and (2) determination of the effect of gene silencing on progeny virion secretion. The RNA of a subgenomic replicon of WNV (lacking complete genes for the capsid, pre-membrane, and envelope proteins) was used for viral translation studies<sup>30</sup>, while a full length viral genome was used for viral secretion studies<sup>31</sup>. The viral RNA was prepared as described previously<sup>31</sup>. The viral RNA was transiently transfected into HeLa cells by electroporation, after gene knock down with siRNA for 3 days. Mouse hyperimmune

ascitic fluid against WNV was used for the immunofluorescence of replicon transfected cells, after 14 h of transfection. For the viral secretion assay, the culture supernatants were collected at 24 h from HeLa cells electroporated with (400 ng) full length WNV genomic RNA for ERAD silenced cells. As positive control for inhibition of WNV secretion, brefeldin A ( $10 \mu\text{g ml}^{-1}$ ) was used, by adding 12 h post infection. To study the viral release from *MCT4* silenced cells, supernatants were collected at 12 h and 24 h (post-infection), and performed a plaque formation assay. For anti-WNV siRNA (siRNA sequence is given in Supplementary Table 9) treatment of replicon silenced cells, cells are first transfected with anti-WNV siRNA for 6 h, followed by electroporation of replicon, and fixed after 30 h for IFA.

**Inhibitor studies.** HeLa cells were treated with  $15 \mu\text{M}$  MG132 (Biomol) or  $700 \mu\text{g ml}^{-1}$  cycloheximide (Sigma) (dissolved in DMSO) or DMSO for various time periods as described in the text or figure. For determining the role ubiquitination in viral internalization, HeLa cells were pre-treated with MG132 for 1 h, TRITC-WNV was added (m.o.i.  $\approx 100$ ), incubated for 1–4 h at  $37^\circ\text{C}$ , fixed with 4% paraformaldehyde, and confocal microscopy was performed. For determining the post-entry requirements of ubiquitination, the virus was inoculated (m.o.i.  $\approx 0.3$ ), incubated at  $37^\circ\text{C}$ , and MG132 was added at different time points. The cells were fixed and immunostained after 18 h. The final DMSO concentration was no more than 0.2% of the total culture medium.

**Vesicular stomatitis virus (VSV) and HIV studies.** The human immunodeficiency virus (VSV-G carrying pHXBGFP-IRES-nef, an infectious molecular clone expressing GFP; gift of P. Shankar) infection experiments were done by infecting gene silenced cells at an m.o.i. of 0.3 for 24 h, followed by fluorescent imaging (10×, Zeiss) to quantify the percentage infection. For the VSV experiments, cells were pre-treated for 1 h with either DMSO or  $15 \mu\text{M}$  MG132, followed by infection with VSV expressing GFP (m.o.i.  $\approx 0.5$ ) for 12 h. GFP-positive VSV cells were quantified by flow cytometry.

**WNV entry and colocalization studies.** Modification of a previous protocol was used for these studies<sup>32</sup>. Purified virus was exchanged into phosphate buffered saline (PBS, pH 7.4) through repeated cycles of concentration by centrifugation (800g) and dilution with PBS, using 15 ml ultrafiltration tubes (10kD, Amicon). The virus in PBS (equivalent to 0.5 mg per ml protein) was incubated with tetramethyl rhodamine isothiocyanate (TRITC, Pierce Biotechnology) ( $0.3 \text{ mg ml}^{-1}$ , in dimethyl formamide) for 1 h at room temperature. After removal of excess dye, labelled virus (WNV-TRITC) was immediately used for experiments. Labelling did not abolish viral infectivity. Infectious entry of WNV-TRITC was sensitive to the vATPase inhibitor bafilomycin, and colocalized with Rab5 labelled compartments, similar to the entry mechanism of unlabelled WNV (Supplementary Fig. 14a, b). For colocalization imaging, Rab5-GFP or Rab7-GFP transduced HeLa cells were used (gift from T. Dragic). For the entry assay (or Rab5/7-GFP colocalization experiments), cells in 48-well culture plates were transfected with siRNA for 48 h, and re-plated onto glass slide bottom chambers (MatTek) in DMEM (with 5% serum and 20 mM Hepes, pH 7.4). After further 24 h, WNV-TRITC (m.o.i.  $\approx 100$ , to capture sufficient events) was added to the cells and allowed to bind for 1 h at  $4^\circ\text{C}$ , and cells were shifted to  $37^\circ\text{C}$  for different time periods, fixed with 4% paraformaldehyde, and confocal imaging was performed, on a LSM 510 confocal microscope equipped with a Zeiss axiovert 100 M base, using 100× oil objective (Zeiss MicroImaging). Z-stack imaging was done at  $0.5 \mu\text{m}$  sections. Virus particles within the cells were counted using the software velocity and ImageJ.

**Enrichment analysis of biological process and molecular function categories.** Genes were classified into biological process and molecular function terms using the PANTHER system. To assess the statistical enrichment or over-representation of these categories for the set of hits relative to the global set of genes examined in the RNAi screen, *P* values were computed using the hypergeometric probability distribution, which was implemented in the R language (<http://www.r-project.org/>). The hypergeometric distribution describes the probability of finding *s* genes associated with a particular category, in a set of *g* genes essential for WNV infection (identified from the RNAi screen), given that there are *S* genes associated with that same category in the global set of *G* genes examined in the genome-wide RNAi screen. For each category *c*, and the list of genes *l*, the *P* value was calculated as:

$$P(c, l) = 1 - \sum_{k \in \{0, 1, \dots, s\}} [C(g, k) C(G - g, S - k) / C(G, S)]$$

The binomial coefficient is of the form  $C(n, r)$ . A *P* value  $< 0.05$  was considered significant. Categories assigned with at least 10 genes are displayed in Fig. 1b, c. A similar approach was used to examine over-representation in Fig. 4a, except that the assessment of enrichment for biological process categories was made relative to their representation among all HSFs identified.

**Analysis of gene expression across 79 tissues.** Microarray data files were obtained from the Novartis GNF human expression atlas version 2 resource, and expression values of 33,689 probe sets from the HG-U133A (Affymetrix) platform and the GNF1H custom chip were analysed. The data set was normalized using global median scaling, and we filtered the data by excluding from the analysis those probe sets with 100% 'absent' calls (MAS5.0 algorithm) across all 79 tissues. The data set was further filtered by setting a minimum threshold value >20 in at least one sample for each probe set and a maximum-mean expression value >100. Hierarchical clustering (centroid linkage method) was performed with Cluster 3.0 using Pearson's correlation as the similarity metric<sup>33</sup>. Z-score transformation was applied to each probeset across all arrays before generating 'heatmaps' for visualization using TreeView<sup>34</sup>.

**Constructing human protein interaction network.** The protein network construction used protein interaction data obtained from the Human Protein Reference Database (HPRD), Biomolecular Interaction Network Database (BIND), Ingenuity pathways database (Mountainview, CA) and functional information from the literature. The network uses graph theoretical representations in which components (gene products) are depicted as nodes and interactions

between components as edges. Graph layout descriptions were written in the Dot language, which implements a multi-dimensional scaling heuristic and uses an iterative solver (Newton-Raphson algorithm) that searches for low-energy configurations to optimize the graph layout when creating a virtual physical model (Spring model) for visualization.

30. Scholle, F. & Mason, P. W. West Nile virus replication interferes with both poly(I:C)-induced interferon gene transcription and response to interferon treatment. *Virology* **342**, 77–87 (2005).
31. Rossi, S. L., Zhao, Q., O'Donnell, V. K. & Mason, P. W. Adaptation of West Nile virus replicons to cells in culture and use of replicon-bearing cells to probe antiviral action. *Virology* **331**, 457–470 (2005).
32. Helenius, A., Kartenbeck, J., Simons, K. & Fries, E. On the entry of Semliki forest virus into BHK-21 cells. *J. Cell Biol.* **84**, 404–420 (1980).
33. Eisen, M. B., Spellman, P. T., Brown, P. O. & Botstein, D. Cluster analysis and display of genome-wide expression patterns. *Proc. Natl Acad. Sci. USA* **95**, 14863–14868 (1998).
34. Saldanha, A. J. Java Treeview — extensible visualization of microarray data. *Bioinformatics* **20**, 3246–3248 (2004).